Journal of Controlled Release 386 (2025) 114122

Contents lists available at ScienceDirect

Journal of Controlled Release

journal homepage: www.elsevier.com/locate/jconrel

Pre-silencing of TNF-α by targeted siRNA delivery mitigates glucocorticoid resistance of dexamethasone in rheumatoid arthritis

Yongjie Sha [a,b], Liang Yang [a], Jingjing Jiang [a], Jun Cao [a], Miao Sun [a], Lichen Yin [c], Zhiyuan Zhong [a,b,*], Fenghua Meng [a,*]

[a] Biomedical Polymers Laboratory, College of Chemistry, Chemical Engineering and Materials Science, and State Key Laboratory of Radiation Medicine and Protection, Soochow University, Suzhou 215123, PR China
[b] College of Pharmaceutical Sciences, Soochow University, Suzhou 215123, PR China
[c] Institute of Functional Nano & Soft Materials (FUNSOM), Jiangsu Key Laboratory for Carbon-Based Functional Materials & Devices, Collaborative Innovation Center of Suzhou Nano Science & Technology, Soochow University, Suzhou 215123, China

ARTICLE INFO

Keywords:
Rheumatoid arthritis
Glucocorticoid resistance
Dexamethasone
TNF-α
Polymersomes

ABSTRACT

Rheumatoid arthritis (RA) is a chronic, progressive inflammatory autoimmune disease marked by relentless synovial inflammation and joint destruction, for which long-term remission remains challenging. Although dexamethasone (DEX) is commonly employed to rapidly control disease activity, its therapeutic effectiveness is often undermined by the development of glucocorticoid resistance (GCR) and cumulative systemic toxicities. Recent insights suggest that TNF-α-driven inflammation not only perpetuates joint pathology but also sustains a molecular landscape that favors GCR, underscoring an urgent need for therapeutic strategies that jointly target inflammatory signaling and steroid sensitivity. Here, we report a nanomedicine-enabled sequential therapy, in which TNF-α specific siRNA (siTNFα) and DEX are separately encapsulated within macrophage-targeted polymersomes (MTP-T and MTP-D, respectively). Through intravenous administration of MTP-T, followed by the intraperitoneal delivery of MTP-D (designated as MTP-T/D(seq)), this sequential therapy acheives efficient knockdown of TNF-α in inflammatory macrophages, leading to enhanced expression of glucocorticoid receptor (GR), an elevated GRα/GRβ ratio, and a substantial reversal of GCR. This modulation sensitizes macrophages to DEX, enabling rapid and effective suppression of pro-inflammatory mediators while reducing toxicity. Our findings demonstrate that our sequential therapy in collagen-induced arthritis (CIA) mouse models not only mitigates joint inflammation and mitochondrial dysfunction but also normalizes the M2/M1 macrophage balance, attenuating synovial hyperplasia and cartilage damage as confirmed by molecular and histological analyses. These findings validate a precision-engineered immune microenvironment remodeling strategy that restores glucocorticoid responsiveness and confers potent therapeutic benefits, offering a compelling blueprint for overcoming steroid resistance in RA.

1. Introduction

RA is a chronic autoimmune disease characterized by persistent synovial inflammation and progressive damage in joints, bones and surrounding soft tissues [1]. Significant progress has been made with disease-modifying anti-rheumatic drugs (DMARDs) and biologic therapies, such as methotrexate, JAK inhibitors (e.g., tofacitinib and upadacitinib), and monoclonal antibodies targeting cytokines (e.g., adalimumab and etanercept for TNF-α, tocilizumab for IL-6). These agents are widely used in clinical practice and act by disrupting key inflammatory pathways [2,3]. However, their long-term use is frequently limited by heterogeneous clinical responses, sustained immunosuppression with increased infection and malignancy risk, frequent relapses, adverse effects, loss of efficacy, and limited accessibility due to high cost and the need for frequent injections. For example, first-line TNF-α inhibitors such as Humira (adalimumab) may still fail to induce durable remission in a substantial proportion of patients. Similarly, SKYRIZI (risankizumab), though approved for diseases including

* Corresponding authors at: Biomedical Polymers Laboratory, College of Chemistry, Chemical Engineering and Materials Science, and State Key Laboratory of Radiation Medicine and Protection, Soochow University, Suzhou 215123, PR China
E-mail addresses: zyzhong@suda.edu.cn (Z. Zhong), fhmeng@suda.edu.cn (F. Meng).

https://doi.org/10.1016/j.jconrel.2025.114122
Received 28 May 2025; Received in revised form 25 July 2025; Accepted 11 August 2025
Available online 12 August 2025

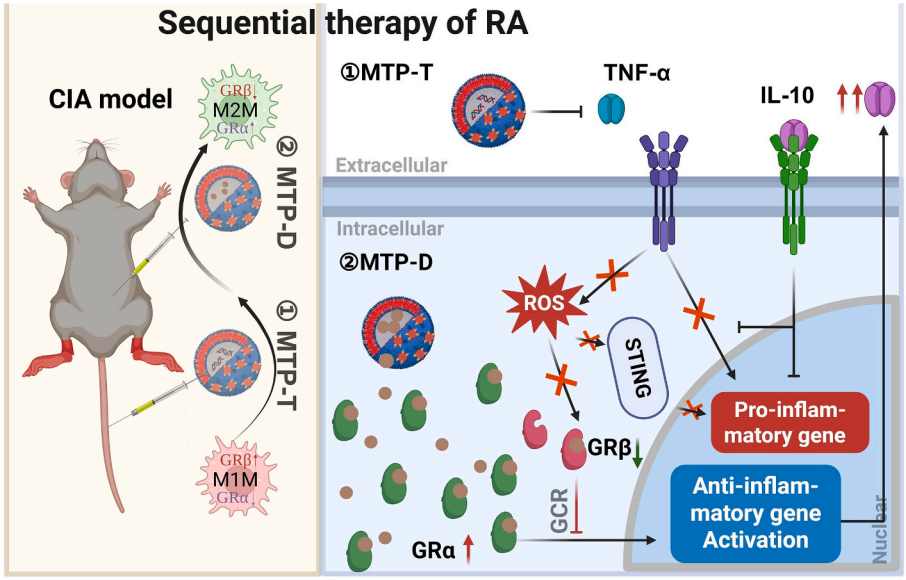

Scheme 1. Illustration of the sequential administration of macrophage-targeted siRNA-encapsulated polymersomes (MTP-T), followed by DEX-loaded polymersomes (MTP-D) synergistically alleviated the inflammation in CIA mouse models.

psoriasis and Crohn's disease, is currently not indicated for RA. Glucocorticoids, exemplified by dexamethasone (DEX), remain integral to both early and advanced RA management for their potent anti-inflammatory effects [4]. Nevertheless, its prolonged use is often associated with adverse effects, including osteoporosis, metabolic disturbances, and increased infection risk [5].

A growing body of evidence implicates glucocorticoid resistance (GCR)—driven in part by sustained inflammatory signaling pathways, especially those mediated by TNF-α [6]—in the loss of therapeutic efficacy and the heightened need for escalated doses, further aggravating toxicity [7]. Impaired glucocorticoid receptor (GR) signaling not only diminishes DEX function [8] but also perpetuates synovial inflammation, creating a vicious cycle that existing therapies fail to disrupt. Emerging combination therapies have sought to restore glucocorticoid responsiveness by targeting upstream inflammatory mediators in various inflammatory contexts [9,10]. Approaches such as anti-TNF-α antibodies, GR modulators, and cytokine pathway inhibitors have demonstrated potential in animal models and early clinical trials [11,12]. For instance, an anti-TNF-α-GCR modulator conjugate such as ABBV-3373 showed sustained anti-RA effect compared to monotherapies [13], yet clinical translation remains hampered by insufficient selectivity, systemic toxicity, and inadequate temporal coordination for effective immune modulation and GR restoration.

Recent advances in nanomedicine offer a compelling strategy to overcome these limitations. Engineered nanocarriers can encapsulate DEX for preferential delivery to inflamed tissues, improving pharmacokinetics, reducing off-target effects [14,15], and enabling long-term therapeutic action at lower doses [16]. Targeted nanosystems, with targeting ligands directing particles to activated macrophages or inflamed endothelium [17,18], have further enhanced local drug accumulation [19], while stimuli-responsive nanosystems allow for controlled and disease-triggered release. In parallel, small interfering RNA (siRNA) technology have enabled a prolonged and specific gene silencing [20], though efficient and selective delivery into target immune cells in vivo remains a critical challenge.

Despite these advances, few studies have directly addressed the mechanisms underlying GCR or integrated temporally coordinated, cell-specific targeting to break the cycle of glucocorticoid insensitivity in RA. In this study, we develop a sequential strategy centered on pre-silencing TNF-α via macrophage-targeted siRNA delivery, followed by administration of DEX-loaded polymersomes (Scheme 1). We leverage tetra-mannose-modified, disulfide-crosslinked polymersomes to ensure high payload stability [21], efficient macrophage-targeting [22], and controlled cytoplasmic release of both siTNFα and DEX. Our findings demonstrate that this sequential nanomedicine approach not only synergistically achieves potent inflammation control and immune microenvironment reprogramming, but also overcomes GCR, diminishes toxicity and extends therapeutic remission in CIA models—the gold standard for preclinical RA research due to their close resemblance to the disease course observed in clinical RA patients. The present study for the first time discloses the mechanism and therapeutic timing of combining siTNFα with DEX to overcome glucocorticoid resistance in RA. This approach has the potential to prolong glucocorticoid treatment cycles, promising for long-term RA management.

2. Experimental section

2.1. Preparation of MTP-D and MTP-T

Macrophage-targeted polymersomes (MTP) encapsulating either DEX or siTNFα, designated as MTP-D and MTP-T, respectively, were co-formulated by adding 100 μL a mixed polymer solution in DMF (40 mg/mL) into a 900 μL HEPES solution (5 mM, pH 6.0) containing either DEX or siTNFα. The mixed polymer was made of poly(ethylene glycol)-*b*-poly (trimethylene carbonate-*co*-dithiolane trimethylene carbonate)-b-spermine (PEG-P(TMC-DTC)-Sper) and tetra-mannose conjugated polymer TM-PEG-P(TMC-DTC) (9/1, molar ratio). After mild stirring (400 rpm, 5 min) and standing still overnight at room temperature, polymersomes were purified by dialysis in phosphate buffer (PB, pH 7.4) for 6 h with hourly exchanges of medium. Non-targeting P-D and P-T were prepared similarly but without TM-PEG-P(TMC-DTC).

2.2. In vitro cellular uptake and cytotoxicity assays toward macrophages

BMDMs or RAW264.7 cells were seeded in a 12-well plate (5×10^5 cells/well) and subsequently pretreated with PBS (M0M, non-treated), with LPS (100 ng/mL)/IFN-γ (20 ng/mL) for 4 h (pro-inflammatory phenotype, M1M), or with IL-4 (20 ng/mL) for 24 h (anti-inflammatory phenotype, M2M) for later in vitro studies.

To study the cellular uptake by various phenotypes of macrophages, cy5-labeled MTP-D and non-targeting counterpart P-D were added at a concentration of 0.2 μg cy5/mL ($n = 3$). After a 4-h incubation, cells

were collected and measured using flow cytometry.

To study the cytotoxicity toward M1M and M2M, pre-stimulated RAW264.7 cells in 96-well plate (3×10^3 cells/well) were treated with MTP-T, MTP-D, their simultaneous co-administration (denoted as MTP-T/D(sim)), or sequential administration of MTP-T and MTP-D (denoted as MTP-T/D(seq)) ($n = 4$). For MTP-T/D(seq) group, MTP-T was added to cells and incubated for 8 h before the addition of MTP-D. For monotherapies, MTP-T and MTP-D was respectively added to cells using the same dosing scheme as in the MTP-T/D(seq) for MTP-T and MTP-D. For MTP-T/D(sim) group, both MTP-T and MTP-D were added to cells at the same time as for MTP-D in MTP-T/D(seq). The concentrations of DEX or siTNFα in the monotherapies were 0, 0.1, 1, 5, 10, 25, 50 μg/mL. For MTP-T/D(sim) group and MTP-T/D(seq), DEX was set to 10 or 30 μg/mL, and siTNFα was added at siTNFα/DEX mass ratio of 0/1, 0.2/1, 0.4/1, 0.8/1, and 1.6/1. After incubation, cells were collected and cell viability was determined using MTT assays.

2.3. Cytokine secretion, disease-associated gene expression and repolarization of M1M

BMDMs seeded in 12-well plates (5×10^5 cells/well) were stimulated with LPS (100 ng/mL)/IFN-γ (20 ng/mL) for M1M for the following studies. Cells were then treated with PBS, MTP-D (10 μg DEX/mL), MTP-T (4 μg siTNFα/mL), MTP-T/D(sim) or MTP-T/D(seq) (4 μg siTNFα/mL, and 40, 20, 8, 4, 2 μg DEX/mL), using PBS and IL-4 (20 ng/mL) treated groups as controls (total $n = 9$). After 24 h incubation, culture media was collected to measure the levels of cytokines (TNF-α, IL-6, IL-10, IFN-α, IFN-β and IFN-γ) using ELISA, and cells were collected and ultrasonically disrupted to determine intracellular proteins GRα and GRβ using ELISA ($n = 3$). One third of the cells were treated with RNA extraction reagent to analyze the mRNA expression of inflammatory-related genes (TNF-α, IL-1β, IL-6, IL-10 and TGF-β), and GCR-related genes (GRα, GILZ and GITRL) using qRT-PCR ($n = 3$). The rest cells were labeled with anti-CD11b, anti-F4/80, anti-iNOS and anti-CD206 antibodies, and measured using flow cytometry to determine the contents of M1M ($CD11b^+$ $F4/80^+$ $iNOS^{high}$) and M2M ($CD11b^+$ $F4/80^+$ $CD206^{high}$) ($n = 3$).

2.4. ROS inhibition, mitochondrial damage and lysosomal activity in macrophages

RAW 264.7 cells seeded in 6-well plates (1×10^6 cells/well) were stimulated with LPS (500 ng/mL)/IFN-γ (20 ng/mL) and treated with PBS, MTP-D (10 μg DEX/mL), MTP-T (4 μg siTNFα/mL), and MTP-T/D (seq). After 12 h incubation, cells were separately stained with DCFH-DA (for ROS detection), or PK Mito Red and Picogreen dsDNA Quantitation Reagent (for detection of Mitochondrial Damage), or PK Mito Red and LysoTracker Green DND-26 (for detection of Lysosome Activity) ($n = 3$). The fluorescent images of ROS in cells were observed using inverted microscope and semi-quantified using ImageJ software. The fluorescent images of mitochondria and lysosomes were imaged using HIS-SIM microscope, and semi-quantified using ImageJ.

2.5. In vivo therapeutic efficacy of MTP-T/D(seq) in RA mice

All animal experiments were performed in accordance with the Guidelines for Care and Use of Laboratory Animals of Soochow University (P.R. China) and approved by the Animal Ethics Committee of Soochow University (approval numbers: 202207A0650, 202209A0113). CIA mouse model was established on male DBA/1 J mice (6–8 weeks, 16–18 g) as previously reported and the first injection day of CFA/Col II was designated as day 0 [21]. Mice from the same batch that were not subjected to collagen and adjuvant induction were designated as healthy control. CIA mice were divided into four groups ($n = 6$): PBS, MTP-D, MTP-T, MTP-T/D(seq), using healthy mice as control. At clinical scores of 4–6, mice of MTP-T/D(seq) group were intravenously injected with 200 μL MTP-T (0.5 mg/kg) at 9:00 p.m., followed by intraperitoneal injection of MTP-D (1.25 mg/kg) at next 9:00 a.m. MTP-T and MTP-D in monotherapies were administered into CIA mice using the same dosing scheme as in the MTP-T/D(seq) for MTP-T and MTP-D. Nano formulations were administered every three days for a total of six times. Every two days ankle joints and foot pads were measured using vernier caliper and body weight was monitored. Clinical scores were performed according to the classical rules (**Table S1**). Orbital blood samples were collected after the second dose to assess IL-6 levels ($n = 6$).

On day 50, mice were photographed before sacrificed. Blood samples were collected to evaluate pro-inflammatory (IL-6, TNF-α) and anti-inflammatory factors (IL-10) ($n = 6$). Knee joint and ankle joints from the left hind legs were homogenized for RNA extraction to analyze mRNA levels (IL-6, IL-10, TNF-α) ($n = 6$). Three diseased knee and ankle cartilage of right hind legs were sliced for H&E and Safranin O-fast green histological analyses ($n = 3$) and GR immunohistochemistry. Histological images were observed using light microscope, and the histopathological scores were obtained according to the scoring table **(Table S2)**. For GR immunohistochemistry images, semi-quantitative analysis was conducted through ImageJ software. One slice of right hind legs from PBS and MTP-T/D(seq) groups were also prepared for multi-colour immunofluorescence (FITC: iNOS, PE: F4/80, PerCy5.5: Vimentin, APC: CD206) and imaged using Slide Scanner Systems.

2.6. Statistical analysis

All data were presented as means ± SD unless otherwise stated. Statistical analysis of differences among groups was performed by one-way ANOVA using Tukey's post-test in GraphPad Prism. * $p < 0.05$ ** $p < 0.01$, *** $p < 0.001$ and **** $p < 0.0001$.

3. Results and discussion

3.1. Preparation of macrophage-targeted polymersomes encapsulating DEX or siTNFα

To achieve precise and efficient delivery of therapeutic agents to inflamed joints, we engineered macrophage-targeted polymersomes (MTP) encapsulating either dexamethasone (DEX) or siRNA against TNF-α (siTNFα), designated as MTP-D and MTP-T, respectively. MTP-D and MTP-T were prepared via the self-assembly of copolymer PEG-P(TMC-DTC)-spermine, and co-formulated with 10 mol% of tetra-mannose conjugated PEG-P(TMC-DTC) in an aqueous buffer containing either DEX or siTNFα. The incorporation of tetra-mannose facilitated selective binding to mannose receptors highly expressed on activated inflammatory macrophages, a key driver of RA pathology [21,23]. The chimeric polymersome architecture allowed for robust encapsulation of diverse therapeutic cargos, resulting in high drug loading contents achieved were 14.69 ± 0.53% for DEX and 2.39 ± 0.03% for siTNFα (**Table S3**). Such high capacities are attributable to the strong electrostatic interactions between the anionic nature of both DEX and siRNA and the cationic spermine domains, consistent with recent advances [24]. The sizes of MTP-D and MTP-T ranged from 55 to 65 nm, with size distribution (PDI) of 0.1–0.2 (**Fig. S1a**), signifying uniform nanoparticle fabrication and favorable pharmacokinetic properties for tissue penetration. Nanoparticles exploit the ELVIS (Extravasation through Leaky Vasculature and subsequent Inflammatory cell-mediated Sequestration) effect in inflamed joints, and a size range of 55–65 nm ensures enhanced accumulation while minimizing rapid clearance [25]. These polymersomes displayed excellent colloidal stability both after a 50-fold dilution or during storage at 4 °C for at least 4 weeks, with minimal drug leakage over 2-week period (**Fig. S1b, c**). Notably, in phosphate buffer (PB) containing 10 mM GSH, reflecting the intracellular reductive environment of inflammatory macrophages in RA tissues, over 80% of the encapsulated drug was liberated within 24 h (**Fig. S1d, e**), confirming a GSH-responsive release mechanism.

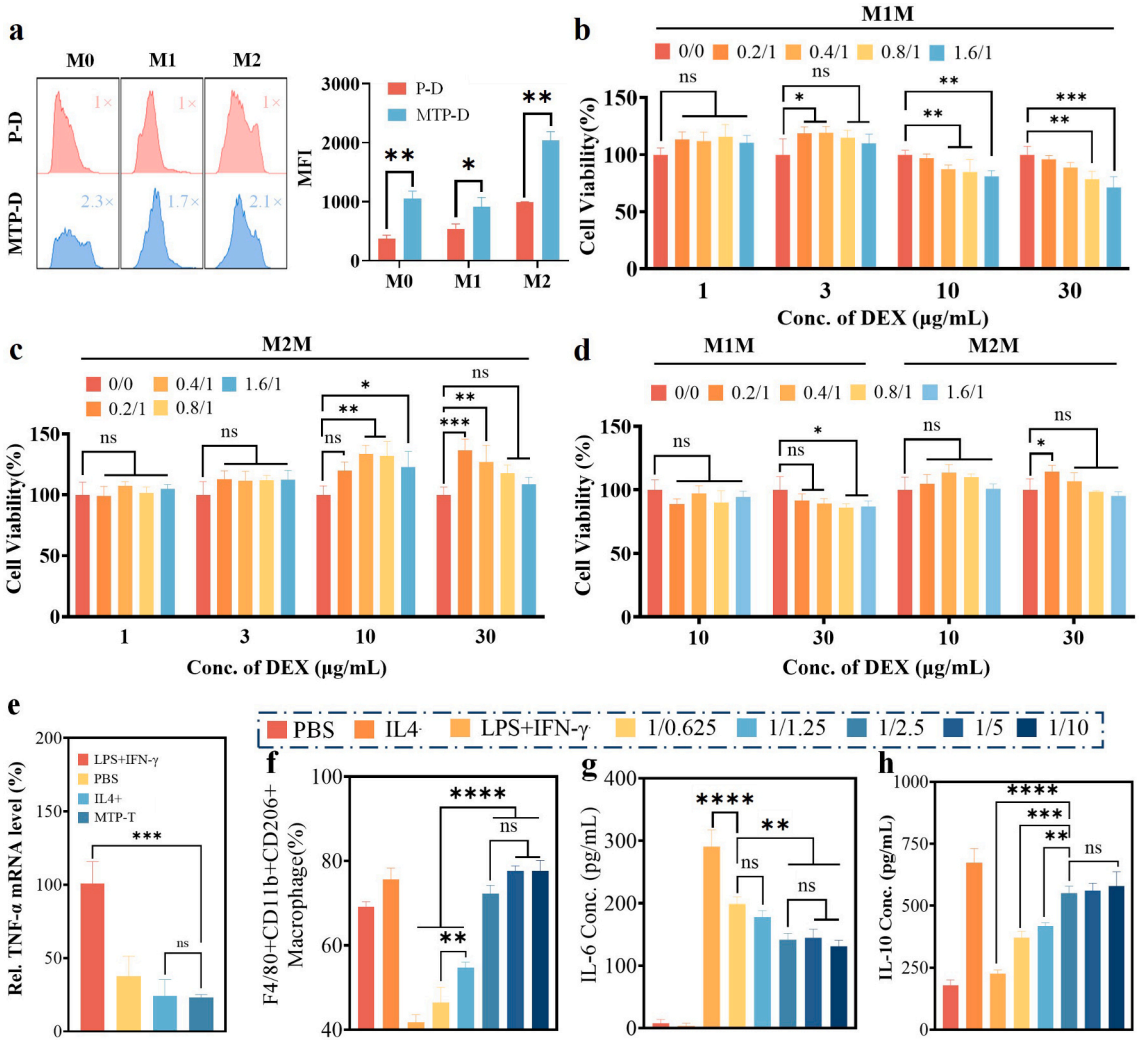

Fig. 1. Cellular studies of MTP-D and MTP-T on macrophages. (a) Uptake of Cy5-labeled MTP-D by M0, M1 and M2 phenotypes of BMDM and semi-quantification analysis ($n = 3$). Viability of (b) M1 and (c) M2 phenotypes of RAW2643.7 cells by sequential addition of MTP-T (4 h incubation) followed by MTP-D (MTP-T/D(seq)) (20 h incubation) at various siTNFα/DEX ratios and fixed DEX concentrations as indicated. (d) Viability of M1M and M2M of RAW264.7 cells treated 24 h with simultaneous addition of MTP-T and MTP-D (MTP-T/D(sim)) ($n = 4$). (e) TNF-α mRNA levels in BMDM treated with MTP-T at siTNFα of 4 μg/mL. (f) M2M proportions in BMDMs and concentrations of (g) IL-6 and (h) IL-10 secreted by BMDMs treated with MTP-T/D(seq) for 24 h with various siTNFα/DEX ratios ($n = 3$).

3.2. *In vitro study on macrophage targeting and cytotoxicity*

To assess the macrophage-targeting capability and cytocompatibility of MTP-D and MTP-T, we investigated their uptake and effects across different macrophage phenotypes representative of RA microenvironment. RAW 264.7 macrophages (M0M) were differentiated into either M1 phenotype (M1M, stimulated with LPS and IFN-γ) or M2 phenotype (M2M, stimulated with IL-4). The cy5-labeled MTP-D exhibited distinctly elevated uptake in all three macrophage phenotypes compared to non-targeted control, P-D (Fig. 1a), confirming the efficacy of ligand-driven selectivity. The selectivity was ascribable to the high-affinity interaction between multivalent tetra-mannose on polymersomes and CD206, which is overexpressed on macrophages. This targeting is enabled through the cooperative action of C-type lectin domains 5–8, as reported previously [22]. Notably, the highest uptake was observed in M2M, likely due to the enriched expression of mannose receptor CD206 compared to M1M and M0M, in agreement with recent reports [26]. Despite this, within the inflamed synovium of RA, M1M overwhelmingly predominate and drive pathological inflammation, while M2M are sparse at disease onset but can be stimulated to expand during the resolution phase [27]. This prioritization is therapeutically advantageous, as our platform targets the dominant inflammatory cell type in active RA.

Subsequent cytotoxicity assays with MTP-D, free DEX and P-D did not affect the viability of either M1M or M2M at clinically relevant DEX concentrations (DEX conc. $\leq$ 50 μg/mL), and similarly minimal effects were observed in non-macrophage 293 T cells at lower DEX concentration (**Fig. S2, S3a**). Importantly, MTP-T was well tolerated by both M1M and M2M across all tested concentrations (**Fig. S3b**), highlighting the potential for combined gene-silencing and small-molecule regimens with low off-target toxicity. Interestingly, sequential therapy, pretreating M1M with MTP-T follow by MTP-D (MTP-T/D(seq)), elicited the strong cytotoxic effect against M1M, with maximal efficacy at siTNFα/DEX ratios of 0.4/1, 0.8/1 and 1.6/1 (DEX: 10 and 30 μg/mL, Fig. 1b). Conversely, M2M remained unaffected or even exhibited proliferative responses under certain ratios (Fig. 1c). Furthermore, simultaneous co-administration (MTP-T/D(sim)) failed to enhance cytotoxicity compared to the sequential strategy (Fig. 1d), emphasizing the critical importance of temporally coordinating gene silencing with drug delivery.

At the molecular level, quantitative RT-PCR revealed robust down-regulation of TNF-α mRNA in M1M following MTP-T treatment, while effects in M2M were negligible due to their inherently low TNF-α expression (Fig. 1e). In addition, a distinct temporal pattern in TNF-α

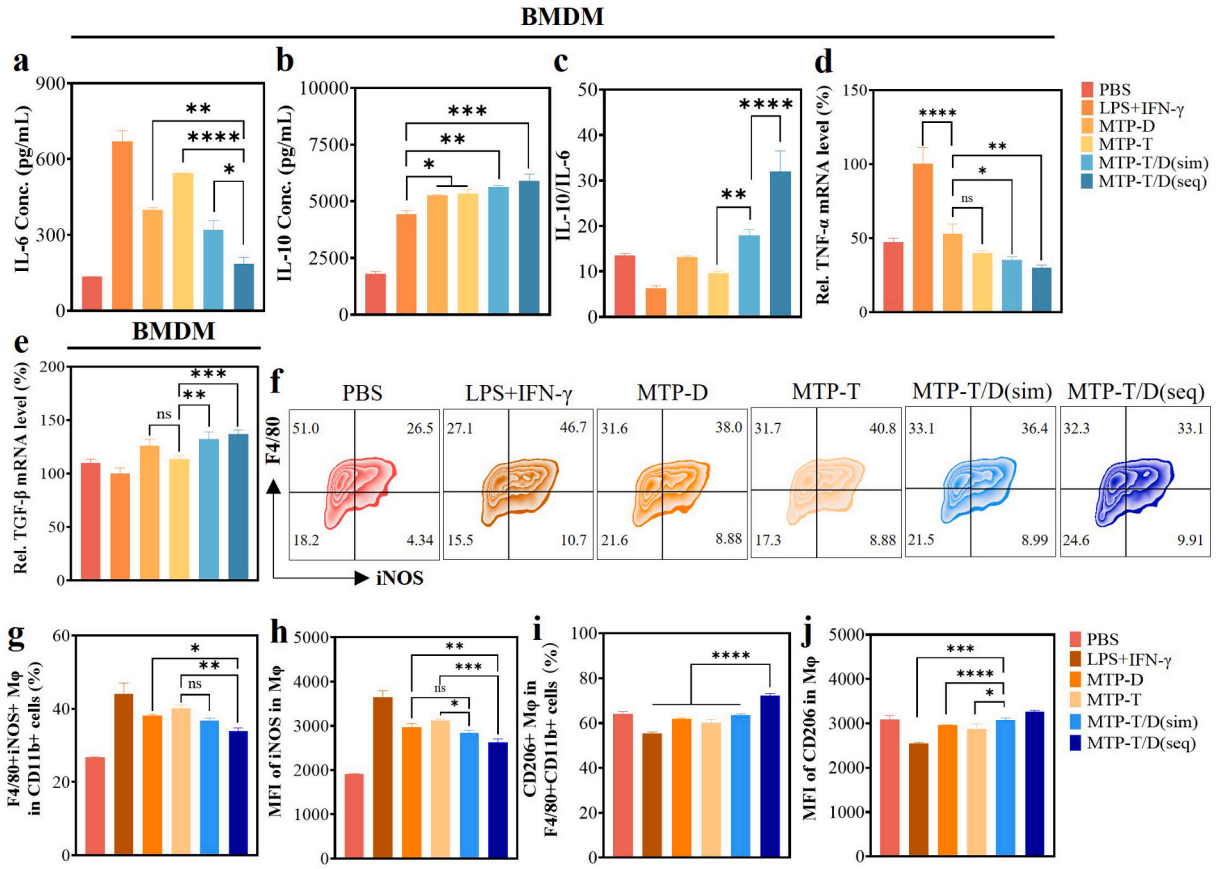

Fig. 2. In vitro studies of anti-inflammation and immunoregulation of MTP-T/D(seq). Concentrations of (a) IL-6, (b) IL-10 and (c) IL-10/IL-6 ratios of BMDM treated with nanoformulations at siTNFα/DEX = 1/2.5 and DEX concentration of 10 μg/mL ($n = 3$). The mRNA levels of (d) TNF-α and (e) TGF-β in BMDM treated with MTP-T/D(seq) at siTNFα/DEX = 1/2.5 ($n = 3$). (f) Representative flow cytometry zebra plots and (g) percentages of M1M, (h) MFI of iNOS expression, (i) percentages of M2M and (j) MFI of CD206 expression of $CD11b^{+}F4/80^{+}$ BMDM ($n = 3$).

mRNA expression was observed, with levels peaking between 4 and 12 h post-stimulation (**Fig. S4a**). While following MTP-T administration, TNF-α mRNA levels (relative to PBS) exhibited a rapid decline from 4 to 12 h, and much more gradual decrease from 12 to 36 h (**Fig. S4b**). These results signify a sustained therapeutic effect of MTP-T and delineate an optimal intervention window (12–36 h) for subsequent MTP-D treatment. These findings suggest that a synergistic mechanism whereby siRNA-mediated pre-silencing of TNF-α potentiates subsequent glucocorticoid signaling in inflammatory macrophages, facilitating both immune rebalancing and repolarization toward a tissue-resolving phenotype.

3.3. In vitro cytokine secretion and macrophage repolarization by the sequential strategy

The inflammatory microenvironment in RA is dominated by classically activated M1M that perpetuate tissue injury via persistent secretion of pro-inflammatory cytokines such as IL-6, TNF-α, and IFN-γ, while suppressing resolution-promoting factors like IL-10 and TGF-β [28]. Therapeutic strategies that can both deplete pathogenic M1M and reprogram their phenotype toward a reparative, M2-like state offer exceptional promise for durable immune modulation. Building on our previous findings of efficient and selective delivery, we assessed immunomodulatory potential of the MTP-T/D(seq) strategy in vitro using LPS/IFN-γ-stimulated BMDM (M1M). Flow cytometry confirmed that pre-silencing TNF-α with MTP-T prior to DEX exposure (MTP-T/D (seq)) effectively downregulated the inflammatory axis. Critically, the MTP-T/D(seq) strategy achieved striking repolarization of M1M toward M2M, with the optimal siTNFα/DEX ratios (1/5 and 1/10) yielding up to ca. 80% $CD206^{+}$ M2M (Fig. 1f)—levels that exceed those reported for direct glucocorticoid or siRNA monotherapies [29,30]. Cytokine assessments revealed that these optimized ratios reduced IL-6 levels while promoting IL-10 secretion (Fig. 1g, h), resulting in highest IL-10/IL-6 ratios among all tested conditions. This enhanced anti-inflammatory index can be recognized as an indicator of clinical benefit in RA interventions [31,32]. Accordingly, the siTNFα/DEX ratio of 1/2.5, considering the balance of efficacy and glucocorticoid sparing, was chosen for subsequent in vivo experiments. Compared to either agent alone or MTP-T/D(sim), MTP-T/D(seq) led to the most pronounced reduction in IL-6, greatest increase in IL-10, and significantly elevated IL-10/IL-6 ratio (Fig. 2a-c, **S5a-c**). These results underscore the importance of temporal orchestration: preconditioning macrophages by TNF-α silencing effectively sensitizes them to subsequent glucocorticoid action, resulting in durable reprogramming of inflammatory responses.

At the transcriptomic level, qRT-PCR results further confirmed that the MTP-T/D(seq) strategy effectively silenced TNF-α and IL-1β mRNA in macrophages while concurrently upregulated genes promoting immune regulation and tissue repair (e.g., TGFβ), outperforming mono- or simultaneous therapies (Fig. 2d-e, **S5d**). The proportion of pro-inflammatory $iNOS^{+}$ M1M was significantly reduced (from 46.7% to 33.1%), while the proportion of CD206+ M2M increased markedly (from 56.1% to 73.2%), as detected by flow cytometry (Fig. 2f-i, **Fig. S6**). This strategic repolarization of the macrophages translated into decreased overall iNOS expression and enhanced CD206 levels in total BMDMs (Fig. 2h-j), evidencing a profound shift toward an anti-inflammatory tissue landscape.

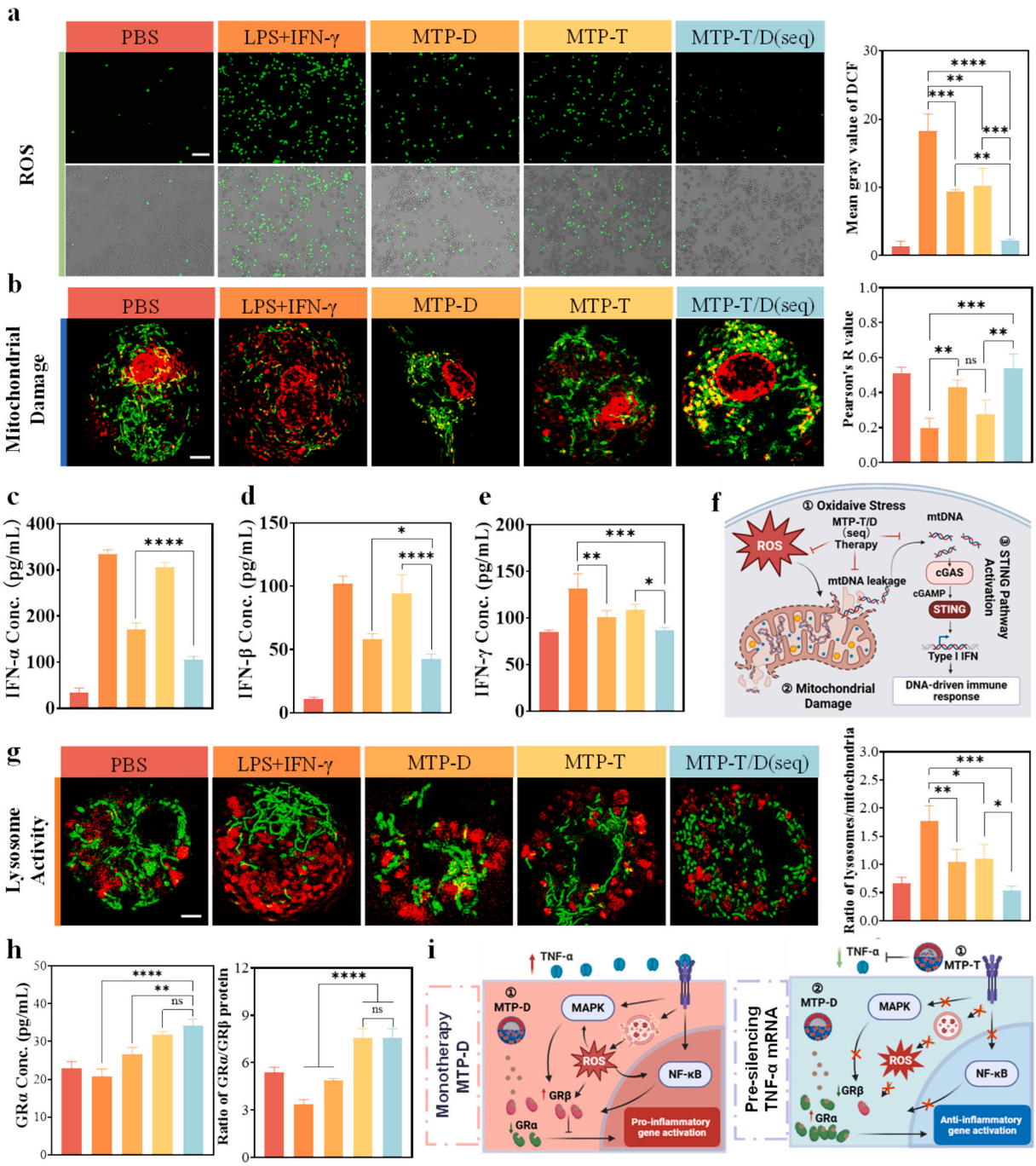

Fig. 3. The MTP-T/D(seq) strategy alleviated oxidative stress and GCR of RAW264.7 cells. (a) Fluorescence images and semiquantification of mean fluorescence intensity of ROS (Scale bar: 100 μm). (b) Fluorescence images of mitochondrion and mtDNA and the Pearson's R value of mtDNA (red) and inner mitochondrial ridge (green) (Scale bar: 2 μm). Production of (c) IFN-α, (d) IFN-β and (e) IFN-γ. (f) Schematic of mitochondria damage and STING activation. (g) Fluorescence images of mitochondria and endolysosomes and the ratio of fluorescence intensity of lysosomes/mitochondria (Scale bar: 2 μm). Study on mechanism of alleviating GCR via MTP-T/D(seq) therapy ($n = 3$). (h) Concentrations of GRα and GRα/GRβ ratios. (i) Schematic of mechanism of pre-silencing TNF-α mRNA alleviating GCR. RAW264.7 cells were stimulated by LPS (100 ng/mL)/IFN-γ (20 ng/mL), and MTP-T/D(seq) was applied by sequential addition of MTP-T (4 h incubation) followed by MTP-D (MTP-T/D(seq)) (20 h incubation) at 4 μg/mL siTNFα and 10 μg/mL DEX. PBS, MTP-D, and MTP-T were used as control samples. (For interpretation of the references to colour in this figure legend, the reader is referred to the web version of this article.)

3.4. Alleviation of oxidative stress and preservation of mitochondrial integrity by MTP-T/D(seq)

Building on the potent immunomodulatory effects observed with the MTP-T/D(seq) strategy, we next explored its impact on oxidative stress and mitochondrial homeostasis—two central components in the perpetuation of chronic inflammation and tissue damage in RA [33,34]. Excessive production of reactive oxygen species (ROS) by M1M disrupts mitochondrial integrity, leading to mitochondrial DNA (mtDNA) fragmentation and leakage, and subsequently activates cytosolic pattern recognition pathways such as STING—amplifying inflammatory signaling [35].

CLSM analysis revealed that LPS/IFN-γ-stimulated M1M displayed markedly elevated ROS levels, as evidenced by robust 2′-7′

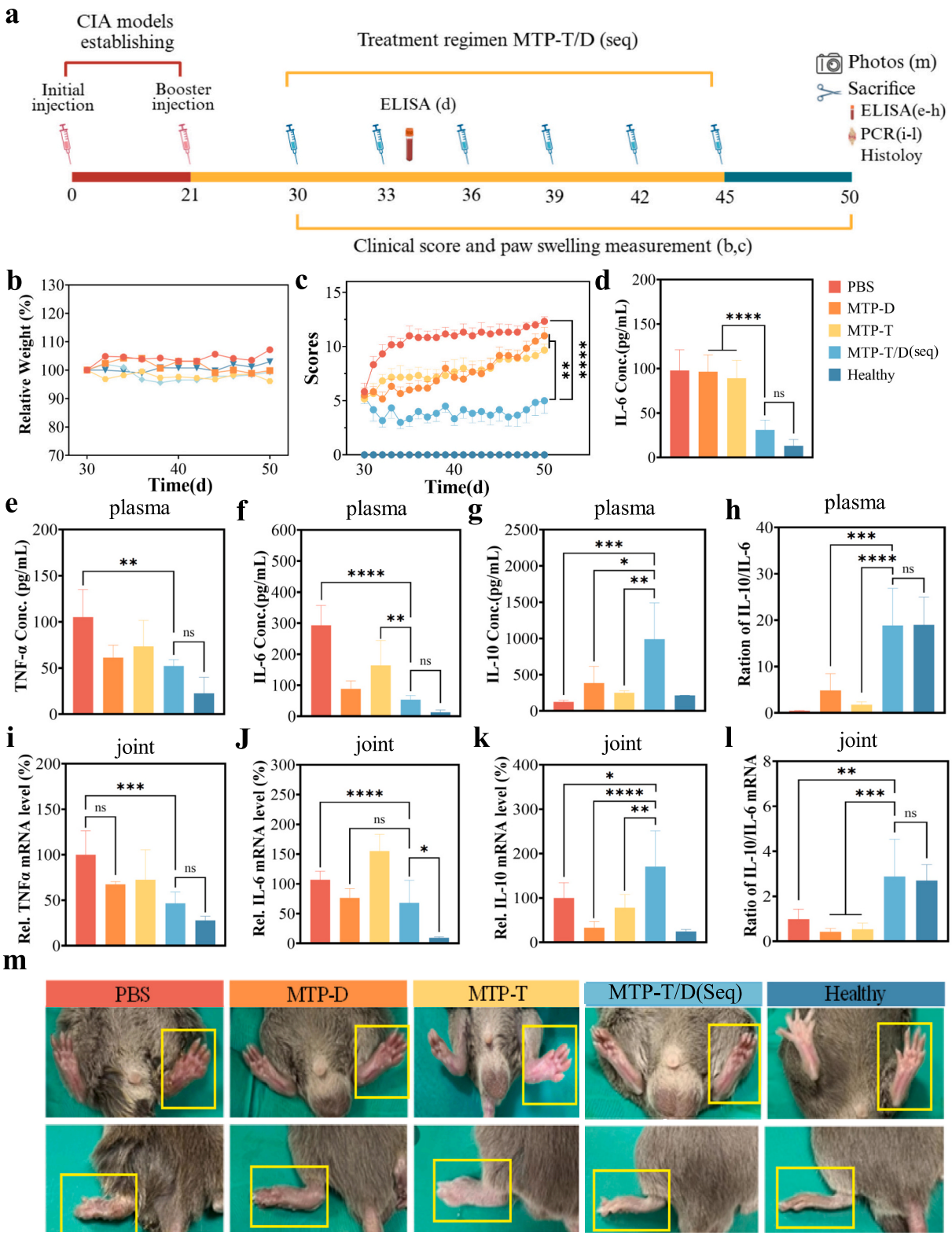

Fig. 4. Anti-RA therapy of MTP-T/D(seq) in CIA models ($n = 6$). (a) Experimental arrangements. (b) Body weight changes and (c) arthritis scores of the mice during treatment. (d) Concentrations of IL-6 in peripheral blood on day 34. Concentrations of (e) TNF-α, (f) IL-6, (g) IL-10, and h) the IL-10/IL-6 ratio in peripheral blood, and relative mRNA expression of (i) TNF-α, (j) IL-6, (k) IL-10, and (l) ratio of IL-10/IL-6 mRNA in ankle joints on day 50, as well as (m) photos of the feet.

dichlorofluorescein fluorescence (Fig. 3a), and significant mitochondrial disorganization (Fig. 3b), showing extensive mtDNA (red) release into cytoplasm [36], a hallmark of cellular stress that propagates auto-amplificatory immune circuits. In contrast, the MTP-T/D(seq) therapy, compared to monotherapies and $LPS^{+}IFN\text{-}\gamma^{+}$-treated controls, significantly reduced intracellular ROS levels and preserved mitochondrial architecture (Fig. 3a, b). MTP-T/D(seq)-treated macrophages, predominantly M2M, exhibited markedly less mtDNA fragmentation and maintained optimal colocalization of mtDNA within structurally intact mitochondria (Fig. 3b), a feature that is strongly associated with

decreased activation of the STING pathway and suppression of interferon responses [37,38]. Aligning with these observations, quantification of IFN subtypes confirmed a significant reduction in their secretion (Fig. 3c-e).

Mechanistically, these findings suggest that the sequential downregulation of TNF-α with targeted siRNA primes macrophages to mount a controlled, rather than exacerbated, response to subsequent glucocorticoid exposure. This not only prevents the vicious cycle of oxidative damage and STING-mediated inflammation but also enables more efficient repolarization toward M2M. The schematic summarizes how MTP-T/D(seq) constrains the feed-forward loop linking mtDNA leakage to innate immune activation (Fig. 3f). Furthermore, improved mitochondrial integrity likely supports enhanced endosomal and lysosomal dynamics, which are crucial for effective metabolism and resolution of cellular debris in chronically inflamed tissues [39]. By mitigating both mitochondrial dysfunction and pro-oxidant signaling, the MTP-T/D(seq) treatment signifies a holistic nanotherapeutic approach: it safeguards organelle function, tempers maladaptive inflammation, and supports immune rebalance through coordinated reprogramming of macrophage state.

3.5. Reversal of GCR in inflammatory macrophages via MTP-T/D(seq) treatment

A significant concern regarding the prolonged clinical use of DEX is the development of GCR, which impairs its anti-inflammatory efficacy. GCR primarily stems from dysregulation within GR signaling axis. Among the molecular hallmarks of GCR are diminished GRα expression and an altered GRα/GRβ ratio, both of which attenuate the ligand-binding and transactivation capacity of GR [40], culminating in reduced sensitivity to steroids [41]. Accumulating evidence suggests that chronic inflammatory cytokine exposure—particularly TNF-α—triggers abnormal lysosomal activation, accelerating the degradation of GRα protein and fostering the imbalance of GRα/GRβ and resistance [42,43]. Our in vitro model experiments demonstrated that LPS/IFN-γ-stimulated M1M exhibited abnormal lysosomal hyperactivity and excessive proliferation, concurrent with a decline in intracellular GRα and a suppressed GRα/GRβ ratio. Crucially, MTP-T/D(seq) treatment profoundly modulated lysosomal dynamics as seen from high-resolution fluorescence images that revealed normalized lysosome abundance (red) and restored mitochondrial–lysosomal homeostasis in MTP-T/D (seq) (Fig. 3g), in accordance with its maintained mitochondrial integrity. ELISA quantification confirmed that MTP-T/D(seq) treatment effectively preserved cellular GRα content and elevated the GRα/GRβ ratio compared to DEX therapy alone (Fig. 3h, **S7a**). A significant increment in GRα mRNA expression was also seen in the MTP-T/D(seq) group (**Fig. S7b**). This enhancement was further reflected in the upregulation of GILZ (**Fig. S7c**), a canonical GRα transcriptional target, indicative of effective receptor activation [44]. Notably, MTP-T/D(seq) strategy boosted GRα mRNA expression by over twofold relative to MTP-D, while also favorably shifting the GRα/GRβ balance.

Moreover, DEX is known to promote the upregulation of glucocorticoid-induced tumor necrosis factor receptor (GITR), a co-stimulatory molecule that enhances effector T cell activation while depleting regulatory T cells (Treg) [45]. Assessment of immune activation markers revealed a 3.7-fold downregulation of GITR ligand (GITRL), a molecule recognized for its role in promoting effector T cell activity and exacerbating tissue inflammation [46], in the MTP-T/D (seq) group **(Fig. S7d)**. The suppression of GITRL by MTP-T/D(seq) may not only dampen the inflammatory response but also indirectly facilitate GR-mediated immunoregulation [47]. These results reveal a mechanistically robust strategy by which sequential TNF-α silencing followed by targeted DEX delivery mitigates the key drivers of GCR (Fig. 3i) at both the protein and transcript levels. By restoring GRα integrity, suppressing hyperactive lysosomal pathways, and dampening auxiliary immune activation signals, the MTP-T/D(seq) platform overcomes steroid resistance that has long undermined the efficacy of glucocorticoid therapy.

3.6. Therapeutic efficacy and immune modulation by MTP-T/D(seq) strategy in CIA models

Encouraged by the promising in vitro evidence for immune reprogramming, oxidative stress mitigation, and reversal of glucocorticoid resistance, we evaluated the in vivo therapeutic efficacy of the MTP-T/D (seq) sequential strategy in the CIA model, a rigorous proxy for human RA. Treatment interventions began at a moderate disease stage (clinical score (CS): 4–6), mirroring early active stage in clinical settings. The administration involved intravenous (i.v.) delivery of MTP-T at 9 a.m., followed 12 h later by intraperitoneal (i.p.) injection of MTP-D in each cycle, totaling six treatments initiated on day 30 post-first immunization (Fig. 4a). The administration schedule was designed for optimal pharmacodynamic synergy, accounting for endogenous steroid rhythms and maximizing exposure during periods of heightened immune activity [48,49]. For choosing administration route, we employed i.v. injection of MTP-T followed by i.p. injection of MTP-D. Alternating routes addresses practical dosing considerations and may also reduce immune clearance associated with repeated i.v. injections. The results showed stable body weights across all treatment groups, without noticeable side effects (Fig. 4b). The PBS group exhibited a marked deterioration in arthritis severity, with three to four paws of each mouse displaying severe RA symptoms by day 35 (CS per paw $\geq$3, Fig. 4c). While CSs for the PBS, MTP-D and MTP-T groups were recorded at 11.0, 6.1 and 6.8, respectively, indicating the moderate efficacy of monotherapies in slowing disease escalation. The efficacy of MTP-D was rapid but transient, with rebound and worsening of symptoms upon repeated dosing, highlighting the clinical challenge of acquired GCR. MTP-T alone exhibited a gradual and modest improvement, consistent with controlled but incomplete shutdown of the inflammatory cascade. Strikingly, the MTP-T/D(seq) sequential therapy achieved synergistic, durable disease control (Fig. 4c). Both clinical scoring and paw swelling markedly improved with this regimen compared to all controls, and this effect persisted throughout the observation window (Fig. 4c, d). Biochemical profiling corroborated these outcomes: ELISA of the serum collected on day 50 revealed significant decreases in TNF-α (2.1-fold) and IL-6 (6.7-fold), coupled with 8.3-fold increase in anti-inflammatory IL-10 relative to PBS group (Fig. 4e-g). Additionally, the IL-10/IL-6 ratio was significantly elevated in the MTP-T/D(seq) group, both in systemic circulation and diseased joint tissue, supported by parallel mRNA trends (Fig. 4h-l).

Importantly, gross examination and functional assessment disclosed that MTP-D and MTP-T monotherapies reduced paw swelling, while residual redness and impaired mobility persisted. In contrast, the MTP-T/D(seq) group showed nearly complete resolution of joint swelling and inflammation, with paw appearance and function indistinguishable from healthy controls (Fig. 4m). These results substantiate the superior therapeutic efficacy of the MTP-T/D(seq) strategy in alleviating RA symptoms and restoring normal physiological function in preclinical validation.

3.7. Protective effects of the MTP-T/D(seq) strategy on bone status

Joint destruction and bone erosion are hallmarks of advanced RA, directly correlating with chronic inflammation and irreversible loss of function. To evaluate the protective potential of MTP-T/D(seq) strategy beyond immune modulation, we assessed histological and immunological markers of tissue integrity and inflammation in CIA mice after 50 days of therapy. Comprehensive hxistopathological evaluation of ankle and knee joints was performed using hematoxylin and eosin (H&E) and safranin O-fast green (SO-FG) staining. In the PBS and MTP-T monotherapy cohorts, extensive structural disruption was evident: joint architecture was obliterated, synovial hyperplasia and dense

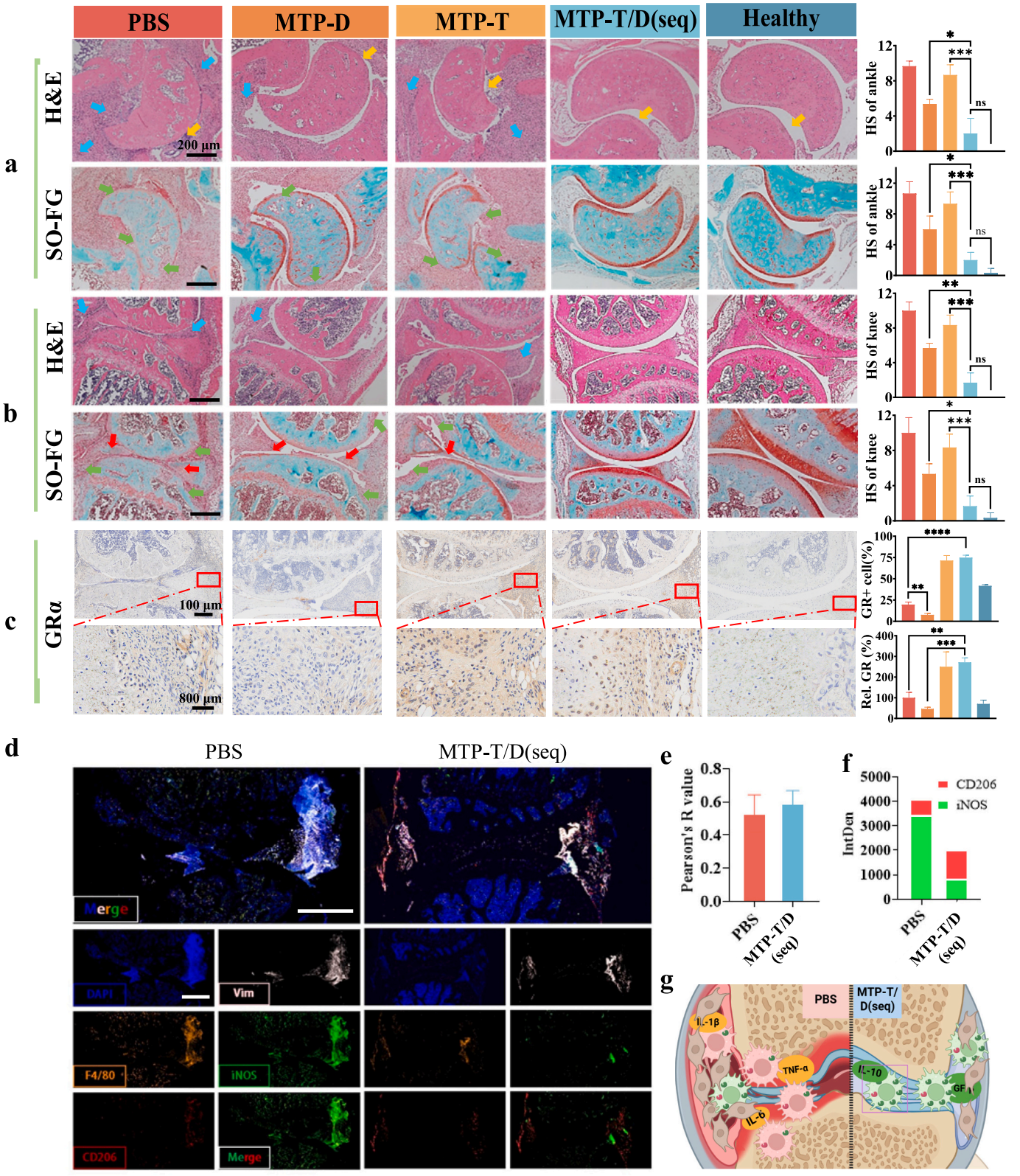

Fig. 5. Histological and immunological analysis of tissue integrity and inflammation of the CIA mice on day 50. Representative pathological images of (a) ankle and (b) knee joints stained with H&E, SO-FG, and their corresponding histological scores (HS). Inflammatory cells (Blue arrow), joint cavity (orange arrow), damaged cartilage structure (red arrow) and degraded meniscus (green arrow) (Scale bar: 200 μm). (c) Representative immunohistochemistry images of GRs in the knee joints, semiquantification of GR expression and GR-positive cell rate. (d) Immunofluorescence images of knee joints treated with PBS or MTP-T/D(seq). Joint tissues were stained with DAPI (nuclei), anti-vimentin (synovium), anti-F4/80 (macrophages), anti-iNOS (M1 macrophages) and anti-CD206 (M2 macrophages) (Scale bar: 200 μm). (e) Pearson's R value between vimentin and F4/80. (f) Integrated total fluorescence density of iNOS (green) and CD206 (red). (g) Schematic of inflammatory microenvironment alleviation following MTP-T/D(seq) treatment. (For interpretation of the references to colour in this figure legend, the reader is referred to the web version of this article.)

inflammatory infiltration predominated (indicated by **blue arrow**), cavities were absent, and soft-tissue adhesions between bone and connective tissue (**orange arrow**) were common (Fig. 5a). Notably, while MTP-D monotherapy alleviated some destruction, it was only the MTP-T/D(seq) regimen that achieved near-complete preservation of native joint and bone morphology. Joints in this group displayed organized synovial lining and sparing of cartilage, closely approximating those of healthy controls (Fig. 5a-b). Quantitative histological scoring (HS) confirmed this superior protection: MTP-T/D(seq) group demonstrated significantly lower scores, indicative of minimal tissue injury.

SO-FG staining substantiated these trends at the cartilage level. In the PBS and MTP-T groups, the cartilage appeared severely damaged (indicated by **green arrows**) and meniscal degradation were widespread with signs of over-fusion. While MTP-D group exhibited partial rescue, with degradation of the meniscus (**red arrows**) and decreased overall staining intensity, likely reflecting underlying bone tissue damage (Fig. 5b). In sharp contrast, the MTP-T/D(seq) group displayed robust cartilage preservation, normal tissue coloration, and negligible meniscal loss, validated by semi-quantitative HS. Mechanistically, immunohistochemical analysis revealed that joints pre-treated with MTP-T (TNF-α silencing) exhibited pronounced upregulation of GR expression—a critical determinant of sustained steroid sensitivity and therapeutic longevity. Sequential addition of MTP-D did not diminish GR expression (Fig. 5c), aligning with findings of durable GCR reversal and prolonged remission observed in this regimen.

Multiplex immunofluorescence provided insight into the impact of the MTP-T/D(seq) strategy on the synovial immune microenvironment. Immunofluorescence staining of knee joint sections used anti-vimentin antibodies to label synovial cells (white) [50], anti-F4/80 for total macrophages (orange), anti-iNOS for M1M (green), and anti-CD206 for M2M (red) (Fig. 5d). CLSM results revealed that iNOS positivity and F4/80+ macrophage infiltration was widespread for PBS group, indicating the devastating M1M-driven inflammation, synovial hypertrophy, and tissue decay. In contrast, joints from the MTP-T/D(seq) group exhibited normalized synovial thickness, significant decrease in total and iNOS+ M1M, and a concomitant increase in reparative $CD206^{+}$ M2M population (Fig. 5e-f). Co-localization analyses further revealed a shift in interactions between macrophages and synovial cells (F4/80 and vimentin) toward a resolution-oriented phenotype—elevated co-localization of M2M with vimentin-expressing synoviocytes and decreased M1M–synovial cell interaction compared to controls (Fig. 5e-f). These findings validate that the MTP-T/D(seq) therapy orchestrates a profound restoration of joint homeostasis (Fig. 5g) in CIA mice by (i) reversing GCR to maximize local steroid activity, (ii) reprogramming the inflammatory microenvironment toward anti-inflammation and tissue repair, and (iii) preventing the downstream cascade of bone and cartilage loss.

4. Conclusions

We have developed a sequential nanomedicine strategy, MTP-T/D (seq), which achieves potent, targeted, and sustained control of RA by precisely manipulating the inflammatory microenvironment. By leveraging a two-step, macrophage-targeted nanovesicle-based delivery platform, our system first deploys siRNA-encapsulated polymersomes (MTP-T) to silence TNF-α and downregulate key inflammatory pathway, thereby effectively reversing GCR and sensitizing pathogenic macrophages to subsequent DEX treatment. This temporal coordination not only enabled robust reduction pro-inflammatory cytokines and restoration of the M1M/M2M balance, but also preserved joint architecture and function in vivo, surpassing the limitations of monotherapies and conventional combination approaches. Mechanistic investigations revealed that the pre-silencing of TNF-α dramatically enhanced GRα expression, minimized lysosomal degradation of the glucocorticoid receptor, and promoted macrophage repolarization toward an anti-inflammatory phenotype—all while constraining oxidative stress and mitochondrial injury. These multifaceted actions translated into durable therapeutic remission and minimal side effects in preclinical models, addressing fundamental challenges in current RA management. By strategically integrating RNAi with advanced nanocarrier engineering and rational sequence design, the MTP-T/D(seq) strategy resolves multidimensional therapeutic resistance and can be adapted for diverse refractory inflammatory and autoimmune diseases in which cytokine-driven steroid resistance play a central role.

Declaration of comepting interest

None.

CRediT authorship contribution statement

Yongjie Sha: Writing – original draft, Methodology, Investigation, Formal analysis, Data curation, Conceptualization. **Liang Yang:** Methodology, Investigation, Formal analysis. **Jingjing Jiang:** Investigation, Formal analysis. **Jun Cao:** Investigation, Formal analysis. **Miao Sun:** Investigation, Formal analysis. **Lichen Yin:** Resources, Methodology. **Zhiyuan Zhong:** Writing – review & editing, Supervision, Resources. **Fenghua Meng:** Writing – review & editing, Validation, Supervision, Project administration, Funding acquisition, Conceptualization.

Acknowledgement

This work is supported by research grant from the National Natural Science Foundation of China (NSFC52033006) and the National Key Research and Development Program of China (2024YFA1210303). The authors thank Biorender.com for the assistance in illustrations (https://BioRender.com/s01f741).

Appendix A. Supplementary data

Supplementary data to this article can be found online at https://doi.org/10.1016/j.jconrel.2025.114122.

Data availability

Data will be made available on request.

References

[1] I.B. McInnes, G. Schett, Pathogenetic insights from the treatment of rheumatoid arthritis, Lancet 389 (2017) 2328–2337.
[2] W. Zhang, Y. Chen, Q. Liu, M. Zhou, K. Wang, Y. Wang, J. Nie, S. Gui, D. Peng, Z. He, Z. Li, Emerging nanotherapeutics alleviating rheumatoid arthritis by readjusting the seeds and soils, J. Control. Release 345 (2022) 851–879.
[3] A. Di Matteo, J.M. Bathon, P. Emery, Rheumatoid arthritis, Lancet 402 (2023) 2019–2033.
[4] M.A. Sacta, Y. Chinenov, I. Rogatsky, Glucocorticoid signaling: an update from a genomic perspective, Annu. Rev. Physiol. 78 (2016) 155–180.
[5] J.N. Hoes, J.W. Jacobs, F. Buttgereit, J.W. Bijlsma, Current view of glucocorticoid co-therapy with DMARDs in rheumatoid arthritis, Nat. Rev. Rheumatol. 6 (2010) 693–702.
[6] S.D. Reichardt, A. Amouret, C. Muzzi, S. Vettorazzi, J.P. Tuckermann, F. Luhder, H. M. Reichardt, The role of glucocorticoids in inflammatory diseases, Cells 10 (2021) 2921.
[7] J. Vandewalle, A. Luypaert, K. De Bosscher, C. Libert, Therapeutic mechanisms of glucocorticoids, Trends Endocrinol. Metab. 29 (2018) 42–54.
[8] J.C. Webster, R.H. Oakley, C.M. Jewell, J.A. Cidlowski, Proinflammatory cytokines regulate human glucocorticoid receptor gene expression and lead to the accumulation of the dominant negative β isoform:: A mechanism for the generation of glucocorticoid resistance, Proc. Natl. Acad. Sci. USA 98 (2001) 6865–6870.
[9] Q. Wang, J. Ren, X. Lin, B. Zhang, J. Li, Y. Weng, Inflammatory stimulus-responsive polymersomes reprogramming glucose metabolism mitigates rheumatoid arthritis, Biomaterials 312 (2025) 122760.
[10] Y. Li, S. Wei, Y. Sun, S. Zong, Y. Sui, Nanomedicine-based combination of dexamethasone palmitate and MCL-1 siRNA for synergistic therapeutic efficacy against rheumatoid arthritis, Drug Deliv. Transl. Res. 11 (2021) 2520–2529.
[11] L. Dejager, K. Dendoncker, M. Eggermont, J. Souffriau, F. Van Hauwermeiren, M. Willart, E. Van Wonterghem, T. Naessens, M. Ballegeer, S. Vandevyver, H. Hammad, B. Lambrecht, K. De Bosscher, J. Grooten, C. Libert, Neutralizing

TNFalpha restores glucocorticoid sensitivity in a mouse model of neutrophilic airway inflammation, Mucosal Immunol. 8 (2015) 1212–1225.
[12] T.J. Creed, C.S. Probert, M.N. Norman, M. Moorghen, N.A. Shepherd, S.D. Hearing, C.M. Dayan, I. Basbuc, Basiliximab for the treatment of steroid-resistant ulcerative colitis: further experience in moderate and severe disease, Aliment. Pharmacol. Ther. 23 (2006) 1435–1442.
[13] M.J. McPherson, A.D. Hobson, A. Hernandez, C.C. Marvin, W. Waegell, C. Goess, J. Z. Oh, D. Shi, M.E. Hayes, L. Wang, L. Wang, D. Schmidt, Z. Wang, V. Pitney, K. McCarthy, Y. Jia, C. Wang, B.N. Kang, S. Bryant, S. Mathieu, M. Ruzek, J. Parmentier, R.R. D'Cunha, Y. Pang, L. Phillips, N.J. Brown, J. Xu, C. Graff, Y. Tian, K.L. Longenecker, W. Qiu, H. Zhu, W. Liu, P. Zheng, Y. Bi, R. Stoffel, An anti–TNF–glucocorticoid receptor modulator antibody-drug conjugate is efficacious against immune-mediated inflammatory diseases, Sci. Transl. Med. 16 (2024) eadd8936.
[14] Y. Deng, H. Zheng, B. Li, F. Huang, Y. Qiu, Y. Yang, W. Sheng, C. Peng, X. Tian, W. Wang, H. Yu, Nanomedicines targeting activated immune cells and effector cells for rheumatoid arthritis treatment, J. Control. Release 371 (2024) 498–515.
[15] H. Liu, M. Ji, Y. Qin, Y. Sun, H. Wang, P. Xiao, J. Zhao, Y. Deng, Z. Zhang, J. Gou, T. Yin, H. He, G. Chen, X. Tang, Y. Zhang, Harnessing self-assembled nanoplatform of dexamethasone and α-linolenic acid for high-efficiency inhibition of pulmonary cytokine storm and fibrosis in mice, Nano Today 55 (2024) 102201.
[16] R. Simon-Vazquez, N. Tsapis, M. Lorscheider, A. Rodriguez, P. Calleja, L. Mousnier, E. de Miguel Villegas, A. Gonzalez-Fernandez, E. Fattal, Improving dexamethasone drug loading and efficacy in treating arthritis through a lipophilic prodrug entrapped into PLGA-PEG nanoparticles, Drug Deliv. Transl. Res. 12 (2022) 1270–1284.
[17] R. Ni, G. Song, X. Fu, R. Song, L. Li, W. Pu, J. Gao, J. Hu, Q. Liu, F. He, D. Zhang, G. Huang, Reactive oxygen species-responsive dexamethasone-loaded nanoparticles for targeted treatment of rheumatoid arthritis via suppressing the iRhom2/TNF-alpha/BAFF signaling pathway, Biomaterials 232 (2020) 119730.
[18] R. Mathur, S. Elsafy, A.T. Press, J. Brueck, M. Hornef, L. Martin, T. Schuoerholz, G. Marx, M. Bartneck, F. Kiessling, J.M. Metselaar, G. Storm, T. Lammers, A. M. Sofias, P. Koczera, Neutrophil hitchhiking enhances liposomal dexamethasone therapy of Sepsis, ACS Nano 18 (2024) 28866–28880.
[19] P. Wang, Y. Zhang, H. Lei, J. Yu, Q. Zhou, X. Shi, Y. Zhu, D. Zhang, P. Zhang, K. Wang, K. Dong, J. Xing, Y. Dong, Hyaluronic acid-based M1 macrophage targeting and environmental responsive drug releasing nanoparticle for enhanced treatment of rheumatoid arthritis, Carbohydr. Polym. 316 (2023) 121018.
[20] C. Li, Y.W. Du, H.Z. Lv, J. Zhang, P.Z. Zhuang, W. Yang, Y.Z. Zhang, J. Wang, W. G. Cui, W. Chen, Injectable amphipathic artesunate prodrug-hydrogel microsphere as gene/drug nano-microplex for rheumatoid arthritis therapy, Adv. Funct. Mater. 32 (2022) 2206261.
[21] L. Yang, Y. Sha, Y. Wei, L. Yin, Z. Zhong, F. Meng, Inflammation-targeted vesicles for co-delivery of methotrexate and TNF-α siRNA to alleviate collagen-induced arthritis, Acta Biomater. 195 (2025) 338–349.
[22] M. Paurevic, M.S. Gajdosik, R. Ribic, Mannose ligands for mannose receptor targeting, Int. J. Mol. Sci. 25 (2024) 100–101.
[23] S. Put, S. Schoonooghe, N. Devoogdt, E. Schurgers, A. Avau, T. Mitera, P. De Baetselier, G. Raes, T. Lahoutte, P. Matthys, SAT0075 the use of macrophage mannose receptor-targeting nanobodies and spect imaging to study joint inflammation in mice with collagen-induced arthritis, Ann. Rheum. Dis. 71 (2012) 495.
[24] L. Qu, G. Cui, Y. Sun, R. Ye, Y. Sun, F. Meng, S. Wang, Z. Zhong, A biomimetic autophagosomes-based Nanovaccine boosts anticancer immunity, Adv. Mater. 36 (2024) 2409590.
[25] L. Hanmei, G. Rui, L. Jiaying, W. Yao, Q. Rui, T. Qi, G. Jingyao, Z. Liang, S. Sanjun, Recent advances in nano-targeting drug delivery systems for rheumatoid arthritis treatment, Acta Mater. Med. 2 (2023) 23–41.
[26] A. Singh, S. Chakraborty, S.W. Wong, N.A. Hefner, A. Stuart, A.S. Qadir, A. Mukhopadhyay, K. Bachmaier, J.-W. Shin, J. Rehman, A.B. Malik, Nanoparticle targeting of de novo profibrotic macrophages mitigates lung fibrosis, Proc. Natl. Acad. Sci. USA 119 (2022) e2121098119.
[27] S. Tardito, G. Martinelli, S. Soldano, S. Paolino, G. Pacini, M. Patane, E. Alessandri, V. Smith, M. Cutolo, Macrophage M1/M2 polarization and rheumatoid arthritis: a systematic review, Autoimmun. Rev. 18 (2019) 102397.
[28] N. Jia, Y. Gao, M. Li, Y. Liang, Y. Li, Y. Lin, S. Huang, Q. Lin, X. Sun, Q. He, Y. Yao, B. Zhang, Z. Zhang, L. Zhang, Metabolic reprogramming of proinflammatory macrophages by target delivered roburic acid effectively ameliorates rheumatoid arthritis symptoms, Signal Transduct. Target. Ther. 8 (2023) 280.
[29] R. Liang, Y. Tu, P. Hua, Y. Huang, M. Chen, ROS-responsive micelles co-loaded dexamethasone and pristimerin to restore the homeostasis of the inflammatory microenvironment for rheumatoid arthritis therapy, Chin. Chem. Lett. 36 (2025) 110335.
[30] H. Xie, X. Huang, B. Li, Y. Chen, H. Niu, T. Yu, S. Yang, S. Gao, Y. Zeng, T. Yang, Y. Kang, K. Zhang, P. Ding, Biomimetic Nanoplatform for targeted rheumatoid arthritis therapy: modulating macrophage niches through self-sustaining positive feedback-driven drug release mechanisms, Adv. Sci. 12 (2025) 2416265.
[31] S. Leboube, T. Bochaton, A. Paccalet, C. Crola Da Silva, P. Jeantet, C. Amaz, C. De Bourguignon, Y. Varillon, C. Prieur, D. Tomasevic, N. Genot, G. Rioufol, E. Bonnefoy-Cudraz, N. Mewton, M. Ovize, IL-10/IL-6 serum ratio as a prognosis marker of STEMI, Eur. Heart J. 41 (2020) 1686.
[32] O.J. McElvaney, B.D. Hobbs, D. Qiao, O.F. McElvaney, M. Moll, N.L. McEvoy, J. Clarke, E. O'Connor, S. Walsh, M.H. Cho, G.F. Curley, N.G. McElvaney, A linear prognostic score based on the ratio of interleukin-6 to interleukin-10 predicts outcomes in COVID-19, EBioMedicine 61 (2020) 103026.
[33] T. Yamada, A. Ikeda, D. Murata, H. Wang, C. Zhang, P. Khare, Y. Adachi, F. Ito, P. M. Quirós, S. Blackshaw, C. López-Otín, T. Langer, D.C. Chan, A. Le, V.L. Dawson, T.M. Dawson, M. Iijima, H. Sesaki, Dual regulation of mitochondrial fusion by Parkin–PINK1 and OMA1, Nature 639 (2025) 776–783.
[34] J. Zhang, Y. Wang, M. Fan, Y. Guan, W. Zhang, F. Huang, Z. Zhang, X. Li, B. Yuan, W. Liu, M. Geng, X. Li, J. Xu, C. Jiang, W. Zhao, F. Ye, W. Zhu, L. Meng, S. Lu, R. Holmdahl, Reactive oxygen species regulation by NCF1 governs ferroptosis susceptibility of Kupffer cells to MASH, Cell Metab. 36 (2024) 1745–1763.
[35] X. Liu, H. Zhang, L. Xu, H. Ye, J. Huang, X. Jing, Y. He, H. Zhou, L. Fang, Y. Zhang, X. Xiang, R.D. Cannon, P. Ji, Q. Zhai, Cgamp-targeting injectable hydrogel system promotes periodontal restoration by alleviating cGAS-STING pathway activation, Bioact. Mater. 48 (2025) 55–70.
[36] S. Yu, J. Du, Q. Zhang, Z. Li, S. Ge, B. Ma, Mitochondria-targeted polyphenol-cysteine nanoparticles regulating AMPK-mediated mitochondrial homeostasis for enhanced bone regeneration, Adv. Funct. Mater. 34 (2024) 2402463.
[37] X. Li, X. Chen, L. Zheng, M. Chen, Y. Zhang, R. Zhu, J. Chen, J. Gu, Q. Yin, H. Jiang, X. Wu, X. Ji, X. Tang, M. Dong, Q. Li, Y. Gao, H. Chen, Non-canonical STING–PERK pathway dependent epigenetic regulation of vascular endothelial dysfunction via integrating IRF3 and NF-κB in inflammatory response, Acta Pharm. Sin. B 13 (2023) 4765–4784.
[38] Y.J. Lei, C.G. Martinez, S. Torres-Odio, S.L. Bell, C.E. Birdwell, J.D. Bryant, C. W. Tong, R.O. Watson, L.C. West, A.P. West, Elevated type I interferon responses potentiate metabolic dysfunction, inflammation, and accelerated aging in mtDNA mutator mice, Sci. Adv. 7 (2021) eabe7548.
[39] P. Kakanj, M. Bonse, A. Kshirsagar, A. Gökmen, F. Gaedke, A. Sen, B. Mollá, E. Vogelsang, A. Schauss, A. Wodarz, D. Pla-Martín, Retromer promotes the lysosomal turnover of mtDNA, Sci. Adv. 11 (2025) eadr6415.
[40] G.J. Martinez, M. Appleton, Z.A. Kipp, A.S. Loria, B. Min, T.D. Hinds Jr., Glucocorticoids, their uses, sexual dimorphisms, and diseases: new concepts, mechanisms, and discoveries, Physiol. Rev. 104 (2024) 473–532.
[41] M. Aziz, P. Wang, Glucocorticoid resistance and hyperlactatemia: a tag team to worsen sepsis, Cell Metab. 33 (2021) 1717–1718.
[42] J. Tanaka, H. Fujita, S. Matsuda, K. Toku, M. Sakanaka, N. Maeda, Glucocorticoid- and mineralocorticoid receptors in microglial cells: the two receptors mediate differential effects of corticosteroids, Glia 20 (1997) 23–37.
[43] Y.Z. He, Y. Xu, C.H. Zhang, X. Gao, K.J. Dykema, K.R. Martin, J.Y. Ke, E.A. Hudson, S.K. Khoo, J.H. Resau, A.S. Alberts, J.P. MacKeigan, K.A. Furge, H.E. Xu, Identification of a lysosomal pathway that modulates glucocorticoid signaling and the inflammatory response, Sci. Signal. 4 (2011) ra44.
[44] O. Robert, H. Boujedidi, A. Bigorgne, G. Ferrere, C.S. Voican, S. Vettorazzi, J. P. Tuckermann, L. Bouchet-Delbos, T. Tran, P. Hemon, V. Puchois, I. Dagher, R. Douard, F. Gaudin, H. Gary-Gouy, F. Capel, I. Durand-Gasselin, S. Prévot, S. Rousset, S. Naveau, V. Godot, D. Emilie, M. Lombès, G. Perlemuter, A.-M. Cassard, Decreased expression of the glucocorticoid receptor-GILZ pathway in Kupffer cells promotes liver inflammation in obese mice, J. Hepatol. 64 (2016) 916–924.
[45] F. Wang, B. Chau, S.M. West, C.R. Kimberlin, F. Cao, F. Schwarz, B. Aguilar, M. Han, W. Morishige, C. Bee, G. Dollinger, A. Rajpal, P. Strop, Structures of mouse and human GITR–GITRL complexes reveal unique TNF superfamily interactions, Nat. Commun. 12 (2021) 1378.
[46] M. Kloss, M. Krusch, K.M. Baltz, A. Peterfi, I. Kumbier, L. Kanz, H.R. Salih, The ligand of glucocorticoid-induced TNF receptor is expressed on human macrophages and stimulates Proinflammatory and anti-tumor effector functions, Blood 108 (2006) 1649.
[47] I. Henderson, E. Caiazzo, C. McSharry, T.J. Guzik, P. Maffia, Why do some asthma patients respond poorly to glucocorticoid therapy? Pharmacol. Res. 160 (2020) 105189.
[48] F. Quagliarini, A.A. Mir, K. Balazs, M. Wierer, K.A. Dyar, C. Jouffe, K. Makris, J. Hawe, M. Heinig, F.V. Filipp, G.D. Barish, N.H. Uhlenhaut, Cistromic reprogramming of the diurnal glucocorticoid hormone response by high-fat diet, Mol. Cell 76 (2019) 531–545.
[49] F. Ma, Z. Li, H. Liu, S. Chen, S. Zheng, J. Zhu, H. Shi, H. Ye, Z. Qiu, L. Gao, B. Han, Q. Yang, X. Wang, Y. Zhang, L. Cheng, H. Fan, S. Lv, X. Zhao, H. Zhou, J. Li, M. Hong, Dietary-timing-induced gut microbiota diurnal oscillations modulate inflammatory rhythms in rheumatoid arthritis, Cell Metab. 36 (2024) 2367–2382.
[50] Z.Q. Zhai, F.Y. Yang, W.C. Xu, J.C. Han, G.H. Luo, Y.A. Li, J. Zhuang, H.Y. Jie, X. Li, X.L. Shi, X.A. Han, X.Q. Luo, R. Song, Y.H. Chen, J.H. Liang, S.F. Wu, Y. He, E. W. Sun, Attenuation of rheumatoid arthritis through the inhibition of tumor necrosis factor-induced caspase 3/Gasdermin E-mediated Pyroptosis, Arthritis Rheum. 74 (2022) 427–440.